High Temperatures-High Pressures, Vol. 49, pp. 107–124
Reprints available directly from the publisher
DOI: 10.32908/hthp.v49.855

Surface tension of liquid nickel: Re-evaluated and revised data

ANNA WERKOVITS, THOMAS LEITNER AND GERNOT POTTLACHER*

Institute of Experimental Physics, Graz University of Technology, NAWI Graz, Petersgasse 16, 8010 Graz, Austria

Received: August 20, 2019; Accepted: October 4, 2019.

Nickel is an important component in many alloys, so reliable surface tension data in the liquid phase are essential for simulation processes in the metal industry. First results for surface tension of liquid nickel from our working group by *Aziz et al.* [1], which led to one of the first publication on the topic of our *Electromagnetic Levitation* (EML) setup, delivered unusual high values compared to the literature, which itself covers a wide range. To find the reason for this behaviour the aim of this work was to investigate the surface tension of nickel samples from different suppliers at similar purity grades by the *Oscillating Drop* (OD) technique using the EML setup of the Thermophysics and Metalphysics Group at Graz University of Technology. Since no significant deviations between samples from different suppliers have been found, an extensive literature research according to various experimental and evaluation parameters has been performed. In the course of this investigation, the earlier obtained experimental data of *Aziz et al.* were re-evaluated. Due to gained awareness in evaluating the translational frequency in vertical direction, the mystery of these elevated surface tension results could be solved, so that in the end the originally obtained results of *Aziz* have been drastically decreased through re-evaluation.

Keywords: surface tension, liquid nickel, electromagnetic levitation, oscillating drop technique, thermophysical properties

1 INTRODUCTION

Starting in the 1950ies, surface tension of liquid nickel has been measured with different methods. In recent years, mainly containerless methods such

*Corresponding author: pottlacher@tugraz.at

as *Electromagnetic* (EML) or *Electrostatic Levitation* (ESL) have been used to avoid chemical contact with any interface or crucible as contamination affects the measurement results. Starting in 2010, the Thermophysics and Metalphysics Group at Graz University of Technology also built up an EML device using parts donated from German Aerospace Center (DLR). First results on the measurement of surface tension of liquid nickel from our working group by *Aziz et al.* [1] delivered unusual high values, but *Aziz* also showed that the corresponding data in the literature is highly spreading. During a systematic investigation of the surface tension of the iron-nickel system [2] within our group, it was decided to also re-investigate pure nickel to see whether tiny differences in composition occurring at different manufacturers or other material/experimental parameters could cause such highly spreading results.

The surface tension γ of liquid metals mostly exhibits a linear decrease (negative slope $\frac{\partial\gamma}{\partial T}$) with temperature T. Measurement results are typically given in the following form referenced by the melting temperature T_M:

$$\gamma(T) = \gamma(T_M) + \frac{\partial\gamma}{\partial T}\,(T - T_M) \tag{1}$$

2 MATERIALS AND METHODS

2.1 Experimental and evaluation methods in literature

The experimental methods for the determination of the surface tension of liquid metals can be divided into two classes: Non-containerless and containerless methods. Non-containerless methods have the disadvantage that there is always a physical contact of the sample with a crucible or any surface, that contaminates the sample due to the high temperature and the resulting high chemical reactivity. Methods used in the literature are namely *Sessile Drop* (SD), *Maximum Bubble Pressure* (MBP) and *Dynamic Drop Weight* (DDW). Even when using containerless measurement methods such as *Electromagnetic Levitation* (EML) or *Electrostatic Levitation* (ESL), the sample is not safe from contamination, as it is surrounded by an inert gas atmosphere that always contains some residual oxygen or other surface-active elements that potentially lower the measured surface tension.

EML and ESL are both used in combination with the *Oscillating Drop* (OD) technique that underwent an evolution as denoted in Table 1. The first description (R) of this problem has been found by *Lord Rayleigh* [3] in 1879 under the assumption of a force-free environment, no occurring sample rotation and ideal spherical symmetry. This formula is used today at µg-experiments on the ISS or on parabola flights, but generally not under terrestrial conditions. For terrestrial ESL experiments the *Feng and Beard*

[4] correction that takes the effect of the drop charge Q into account is state-of-the-art since 1990. In 1991, also a comparable formula for terrestrial EML setups has been introduced by *Cummings and Blackburn* [5]. The angular frequency ω_R (Rayleigh frequency) appearing in *Rayleigh*'s equation has to be corrected as the 5-fold degeneracy in $\omega_{l=2,m}$ is removed by earth's gravitational force, sample rotation and the deformation of the sample by the magnetic pressure induced by the levitation coil. The most accurate formula is *CB(5.20)A* (see Table 1), where all five peaks of the spherical harmonic frequencies of fundamental order $l = 2$ have to be assigned and the angular translational frequencies $\omega_{l=1,m}$, named $\omega_{\tau,i}$, have to be determined. If the 5 peaks are identified, but are not able to be assigned explicitly, the formula *CB(5.20)UA* gives an upper limit of the surface tension. Due to the high computing effort and time consumption that is required for performing the peak assignment, *CB(5.20)UA* is sometimes still used today. Under special conditions, e.g. low sample rotation frequencies, the difference to *CB(5.20)A* is not significant. Equations *CB(5.20)* and *CB(6.1)* differ only in the approach of the form of the magnetic field in z-direction B_z (parallel to gravity): B_z is assumed to be constant in *CB(6.1)*

TABLE 1
OD evaluation formulas used in the literature. The ID is composed of the author initials, if available, the equation number in the original publication and if a peak assignment (A, stands for assigned) is performed or not (UA, stands for unassigned)

ID	Author	Ref	Year	Equation	Used in
R	Lord Rayleigh	[3]	1879	$\omega_R^2 = \frac{32\pi}{3}\frac{\gamma}{M}$ with sample mass M	[7]–[10]
FB	Feng & Beard	[4]	1990	$\omega_R^2 = \left(\frac{8\gamma}{r_0^3\rho}\right)\left[1-\left(\frac{Q^2}{64\pi^2 r_0^3\gamma\varepsilon_0}\right)\right]\left[1-F(\gamma,q,e)\right]$ with*	[11]
CB (6.3)	Cummings & Blackburn	[5]	1991	$\omega_R^2 = \frac{3\omega_{max}^2+3\omega_{min}^2+4\omega_{mid}^2}{10} - 2\overline{\omega_\tau^2} \pm \frac{\omega_{max}^2-\omega_{min}^2}{10}$ with†	[6]
CB (6.1)	Cummings & Blackburn	[5]	1991	$\omega_R^2 = \frac{1}{5}\sum_{m=-2}^{2}\omega_{2,m}^2 - 2\overline{\omega_\tau^2}$ with†	[12]
CB (5.20) UA	Cummings & Blackburn	[5]	1991	$\omega_R^2 = \frac{1}{5}\sum_{m=-2}^{2}\omega_{2,m}^2 - \overline{\omega_\tau^2}\left\{1.9+1.2\left(\frac{z_0}{a}\right)^2\right\}$ with†	[1] [13]–[15]
CB (5.20)A	Cummings & Blackburn	[5]	1991	$\omega_R^2 = \frac{1}{5}\left(\omega_{2,0}^2+2\omega_{2,\|\|}^2+2\omega_{2,\|\|}^2\right) - \overline{\omega_\tau^2}\left\{1.9+1.2\left(\frac{z_0}{a}\right)^2\right\}$ with‡‡	[16]

* $q^2 = \frac{Q^2}{16\pi^2 r_0^3\varepsilon_0}$, $e^2 = E^2 r_0\varepsilon_0$ and $F(\gamma,q,e) = \frac{\left[243.31\gamma^2 - 63.14q^2\gamma + 1.54q^4\right]e^2}{176\gamma^3 - 120q^2\gamma^2 + 27\gamma q^4 - 2q^6}$ with the radius of the sample r_0, the density ρ, the vacuum permittivity ε_0 and the applied electric field E.

† $\overline{\omega_\tau^2} = \frac{1}{3}\sum_{i=1}^{3}\omega_{\tau,i}^2$, $z_0 = \frac{g}{2\omega_\tau^2}$ and the radius of the sample in shape of an ideal sphere a.

‡ $\omega_{2,|||} = \frac{1}{2}\left(\omega_{2,-m}+\omega_{2,+m}\right)$ according to *Busse* [17] for rotating samples.

and in *CB(5.20)* it is approximated to change linearly in z. Finally, equation *CB(6.3)* used by *Eckler et al.* [6] also presumes a constant B_z. It is designed for the non-rotating case where only three fundamental peaks are present, so that the bandwidth can be quantified which results from assignment margin.

Until here, frequency related measures are expressed as angular frequencies ω to conform to the original form of the equations in the literature. In the following sections it is more convenient to work with frequencies ν. The conversion can be performed by $\omega = 2\pi\nu$.

2.2 Material

Nickel samples of three different suppliers *Alfa Aesar*, *Goodfellow*, *Sigma Aldrich* with similar purities (metals basis) of 99.995%, 99.99+% and 99.99+% respectively, have been investigated. Article numbers, LOT numbers and fabrication shapes can be found here.[1] All samples had to be trimmed/cut from the initial shapes and before inserted into the experimental chamber, they were cleaned in an ultrasonic bath, immersed in isopropanol. Samples in a mass range[2] of 475 mg ±30%, holding a minimal mass of 360 mg and a maximal mass of 727 mg, have been investigated. Mass losses between (0.0 to 1.4) mg with a mean relative value of 0.1% have been observed. The uncertainty estimation of the measured sample masses has been chosen with 0.5 mg higher than the readability and repeatability of the precision balance due to vague knowledge about mass loss mechanisms during the experiment (see Section 2.3).

2.3 Experimental method, setup and parameter of this study

Surface tension is obtained containerlessly in a terrestrial *Electromagnetic Levitation* apparatus (EML), that is fed by a HF-generator operating at 380 kHz, using the *Oscillating Drop* technique (OD) with the latest assigned equation of *Cummings and Blackburn*, *CB(5.20)A* (see Table 1). For a detailed description of the experimental setup of the EML apparatus, see [2][16][18].

The uncertainty analysis is performed using GUM. All uncertainties are stated in the extended form, using a coverage factor of $k = 2$.

Prior to measuring, the experimental chamber was evacuated to $(2.6 \text{ to } 11.0)\cdot10^{-6}$ mbar. Then a measurement atmosphere, composed of high purity argon and a custom gas mixture of high purity helium including 3.8 vol% of H_2, was created. At an evacuation pressure of $9\cdot10^{-6}$ mbar and a

[1] *Alfa Aesar*: art.#: 42331, LOT#: L29X008, shape: slug.
Goodfellow: art.#: 267074-14G, LOT#: 28, shape: rod.
Sigma Aldrich: art.#: NI007950, LOT#: MKCD1178, shape: rod.

[2] Sample masses have been determined by the precision balance Mettler Toledo AB104-S-A. Readability: 0.1 mg, Repeatability: 0.1 mg.

maximum experimental pressure of 850 mbar, an oxygen partial pressure p_{O_2} about $2 \cdot 10^{-6}$ mbar is estimated.[3]

The temperature acquisition is done based on the one-wavelength pyrometer *Impac IGA 6 Advanced* from *LumaSense*, operating in the bandwidth of $\lambda = (1.45 \text{ to } 1.80)$ µm. For the temperature calibration, the melting plateau with the known melting temperature T_M of 1728 K [19] is used. By this means, the normal spectral emissivity ε, hereinafter simply named emissivity, at the melting plateau can be calculated using *Wien*'s approximation [20] and the raw pyrometer reading T_{pyro}, the speed of light in vacuum c, the Planck constant h and the Boltzmann constant k_B:

$$\varepsilon = \exp\left(\frac{c \cdot h}{k_B \cdot \lambda}\left(\frac{1}{T_M} - \frac{1}{T_{pyro}}\right)\right) \tag{2}$$

Under the assumption of a constant emissivity in the liquid phase, the temperature calibration can be performed using the same formula:

$$T = \left(\frac{1}{T_{pyro}} + \frac{k_B \cdot \lambda}{c \cdot h}\ln(\varepsilon)\right)^{-1} \tag{3}$$

The melting plateau is used for calibration, as the reproducibility of the occurring melting temperatures is higher, which strongly depends on the used heating or cooling rates. At the start of the levitation, heating rates are much more similar than the cooling rates obtained directly before the sample solidification. But as described in Section 2.4 no distinct correlation between $T_{pyro@MP}$ and the heating rate could be verified. If the solidification occurs during a measurement, where the temperature is held stable, $T_{pyro@SP}$ is about 20 K higher than at applying the maximal cooling rate. The higher the cooling rate, the larger the undercoolings that are achieved as heterogeneous nucleation sites have less time to be created.

Mean pyro-reading at melting plateau:

$$\overline{T}_{pyro@MP} = (1046 \pm 9)\ °C = (1319 \pm 9)\ K$$

Mean pyro-reading at solidification plateau:

$$\overline{T}_{pyro@SP} = (1030 \pm 20)\ °C = (1300 \pm 20)\ K$$

To achieve trustable plateaus, the heating rates should be as low as possible. This has not been considered at the experimentation itself, but has been taken into account at the uncertainty analysis with an estimated error of $T_{pyro@MP}$ of 10 K. The error of the temperature reading during a surface tension measurement is obtained statistically and lies typically in the range of (2 to 6) K, which

[3] Calculated from the oxygen concentration of the filling gases, which is for both ≤ 2 ppm-mol, and the reduction of O_2 through a filter by a factor of 10^{-3}.

increases after calibration to a range of (15 to 20) K. In Figure 1, a typical temperature profile of an experiment is depicted.

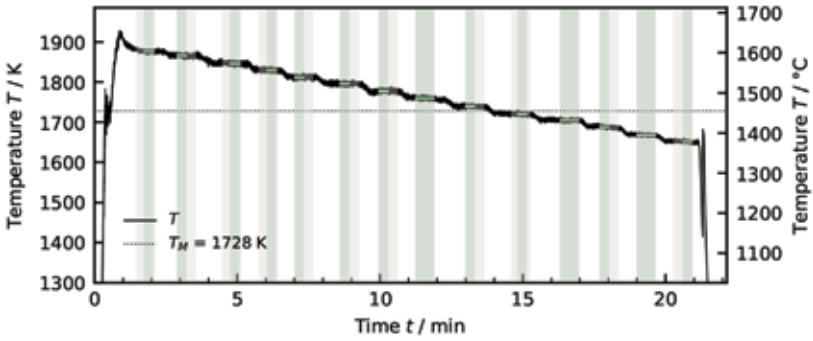

FIGURE 1
Typical temperature profile of measurement series starting at high temperatures until the sample solidifies after stepwise temperature reduction. Green areas show the time range used for surface tension evaluation, whereas grey areas mark the residual measurement time.

The surface tension measurements are performed through the observation of the xy-projection of the levitating sample in the vertical (z-direction) with a high-speed camera using sampling rates of 300 frames per second (fps) and shutter times of mainly 500 µs. At various sample temperatures videos are recorded in order to analyse each single frame by an edge detection algorithm to reduce the information of the frame to the centre of mass coordinates in x- and y-direction and the radii in 5° steps. Afterwards FFTs are performed over those measures to obtain the oscillation frequencies for the OD evaluation formula. Exemplar spectra of an arbitrary radius and the centre of mass coordinates are plotted in Figures 2 and 3, respectively.

As the sample oscillation is only observed in the xy-plane, the translational frequency in the z-direction $\nu_{\tau,z}$ cannot be directly measured through the top camera. But when zooming either in the centre of mass x- or y-coordinate spectra or the R^+ spectra (FFT of R_α+$R_{\alpha+90°}$) a few peaks in the vicinity of the

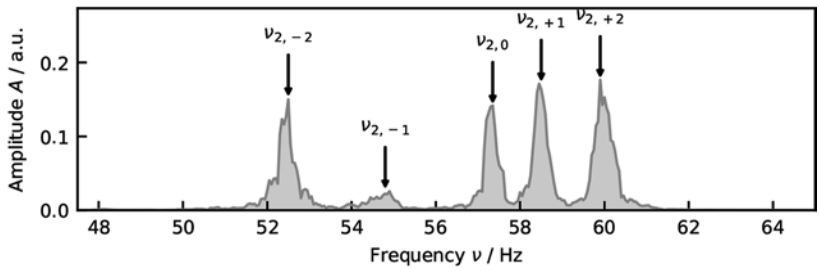

FIGURE 2
Typical frequency spectrum of the sample oscillation at an arbitrary radius in the xy-plane.

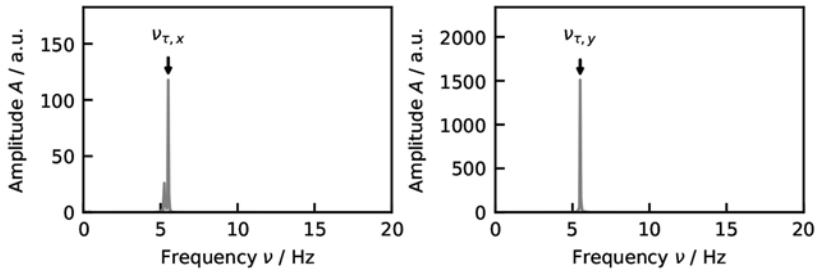

FIGURE 3
Typical frequency spectra of centre of mass coordinates in x- and y-direction (left and right plot respectively).

theoretical value of $\nu_{\tau,z}$, that should be $2{\cdot}\nu_{\tau,x,y}$ according to *Cummings and Blackburn* [5], are visible. In Figure 3, $\nu_{\tau,x} = \nu_{\tau,y} = \nu_{\tau,x,y}$ is 5.6 Hz, so $\nu_{\tau,z}$ should theoretically be at 11.2 Hz. In the centre of mass x-coordinate spectrum in Figure 4 (left), peaks at 11.1 Hz and 12.6 Hz are visible. To exactly determine $\nu_{\tau,z}$, the sample oscillations can be recorded with the side camera, which is normally used for density measurements. Through this direct measurement in Figure 4 (right) it is clear that 12.6 Hz is the quested $\nu_{\tau,z}$. This shift from the ideal $\nu_{\tau,z}$ might result from the unsatisfied assumption of a linearly changing magnetic field in z-direction of the levitation coil or from the 144 Hz duty cycle of the HF-generator. Unfortunately, records of the top and the front camera are not yet synchronized, so just can be performed consecutively at constant temperature. In that way the directly obtained $\nu_{\tau,z}$ can be matched with the indirectly obtained peaks. The directly obtained $\nu_{\tau,z}$ lie in the range of (12.0 ± 0.6) Hz.

At the performed measurements, frequencies $\nu_{l=2,m}$ appear in a range of (35 to 70) Hz with a mean of 58 Hz. Translational frequencies typically appeared in following ranges:

$$\overline{\nu}_{\tau,x} = (5.1 \pm 0.5)\ \text{Hz} \qquad \overline{\nu}_{\tau,y} = (5.2 \pm 0.4)\ \text{Hz} \qquad \overline{\nu}_{\tau,z} = (12.1 \pm 0.6)\ \text{Hz}$$

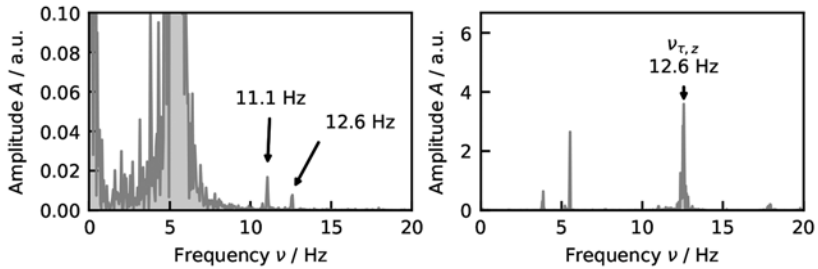

FIGURE 4
Typical frequency spectra of centre of mass coordinates in z-direction. Left: Indirect determination among peak appearance in the spectra of centre of mass x-(here) or y-coordinates or R^+ spectrum. Right: Direct determination.

The similarity of the ranges of indirectly and directly determined $\nu_{\tau,z}$ is a good indicator for a correct peak identification. For the uncertainty analysis the errors of $\nu_{l=2,m}$, $\nu_{\tau,x}$, $\nu_{\tau,y}$ and $\nu_{\tau,z}$ have been estimated by 1 Hz, 0.5 Hz, 0.5 Hz and 0.8 Hz respectively.

For the required density of the OD evaluation the mean of *Nasch and Steinemann* [21], *Chung, Thiessen et al.* [22], *Brillo and Egry* [23], *Schmon, Aziz et al.* (Ohmic pulseheating and EML) [24] and the density measurements performed within this study has been used:

$$\rho_{\text{this study}}(T) = (7750 \pm 20)\cdot\text{kg}\cdot\text{m}^{-3} - (0.7 \pm 0.3)\cdot\text{kg}\cdot\text{m}^{-3}\cdot(T - 1728\ \text{K}) \quad (4)$$

Following, the mean of the chosen literature gives:

$$\overline{\rho}_{\text{lit}}(T) = (7800 \pm 100)\cdot\text{kg}\cdot\text{m}^{-3} - (0.9 \pm 0.5)\cdot\text{kg}\cdot\text{m}^{-3}\cdot(T - 1728\ \text{K}) \quad (5)$$

As only the start (m_s) and end mass (m_e) of the samples at an experiment can be measured, the masses of the single measurements m_i have to be estimated by a model for the mass loss m_{loss} during the experiment. In order to consider the correlation of mass loss and temperature, m_i is calculated from a fraction using integrals over the calibrated temperature T with the starting (t_s) and end time (t_e) of the experiment and the time of the measurement t_i. This gives mainly a quasilinear dependence of m in t:

$$m_i(t_i) = m_s - \frac{\int_{t_s}^{t_i} T\,\mathrm{d}t}{\int_{t_s}^{t_e} T\,\mathrm{d}t}\cdot m_{\text{loss}} \quad (6)$$

In order to strengthen the temperature dependence, the minimal temperature between melting and solidification could be subtracted from the temperature course. Obviously, those approaches act only as a qualitative estimation of the mass loss and there definitely is a need of improvement. *Lee and Matson* [25] introduced *Langmuir*'s equation to calculate the rate of mass evaporation for ESL experiments with pure metals and alloys. As EML experiments operate at nearly atmospheric pressures, which are by a factor of 10^{10} higher than ESL vacuum levels, and a gaseous interfacial layer is induced, the application of the *Langmuir*'s equation would rise in complexity.

The sample deformation amplitude during measurements is typically lower than 5% of the mean radii. According to *Xiao Xiao, et al.* [26], who investigated a nickel-based super alloy[4] using ISS-EML, a deformation amplitude of 5% gives a negative frequency shift of 1%. The quantification of the frequency shift probably cannot be directly adopted, as the sample material

[4] LEK-94 composed mainly of 64% Ni, 15% Al, 7% Co and 7% Cr.

and particularly the definition of the deformation amplitude[5] is not identical for terrestrial and μg EML. For terrestrial EML an observable radial deformation amplitude of 5% in the xy-projection is estimated to be correlated to a total deformation amplitude in the range of (3 to 5)% for the occurrence of mixed modes. This may give a vague estimation of a surface tension increase of 2% when using typical sample and experimental parameter and the worst-case deformation amplitude of 5% and the 1% negative frequency shift.

2.4 Influences of parameter

Figure 5 visualizes the effects, which possibly influence the resulting surface tension. The corresponding estimation of uncertainty contribution is stated in Table 2.

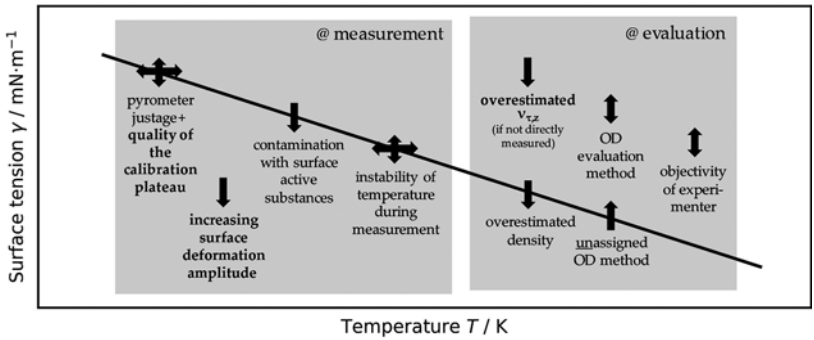

FIGURE 5
Influencing parameter at measurement and evaluation for EML + OD.

TABLE 2
Estimations of extended uncertainties for influencing quantities as presented in Figure 5. Uncertainties are related either to the obtained surface tension or to temperatures

Quantity	Uncertainty contribution
Pyro reading at melting plateau	$\gamma \pm 0.4\%$ (included at fit)
Oxygen contamination	no quantification possible
Surface deformation amplitude	γ + ~2%
Instability of temperature at measurement	$T \pm$ ~5 K, $\gamma \pm 0.1\%$ (included)
Erroneously assigned $\nu_{\tau,z}$	$\gamma_{\mid M} - 8\%$ (at Aziz study, Section 3.3)
Density	$\gamma \pm$ ~0.2 mN·m^{-1} (included)
Unassigned method	$\gamma_{\mid M} + 0.2\%$ (see Section 3.2)

[5] At terrestrial EML all m-modes are excited and not only the $m = 0$ mode as in μg, which causes a well quantifiable deformation along one axis.

The quality of the calibration plateau and the effect of the surface deformation amplitude have been already described in the Sections 2.1 and 2.3. The uncertainty of the calibrated temperature (~20 K) is dominated with the contribution index of 93% by pyro reading of the melting plateau $T_{\text{pyro,M}}$. Initially, a possible dependence of $T_{\text{pyro,M}}$ on the heating rate has been investigated, but no explicit correlation could be verified. Therefore, only an estimation of $T_{\text{pyro,M}}$ inversely influencing the surface tension of ±0.4% or ±6 mN·m^{-1} is made for the highest occurring temperature. A further increase of the quality of the calibration plateau may be only achieved by (besides always ensuring the pyrometer to be well adjusted) low oxide contamination, initial spherical shape and small amplitudes of translational motion. Nevertheless, low heating rates should be aimed. In the introduction, the lowering of the results among contamination with surface-active substances is already explained. This influencing effect can be minimized through a low intrinsic contamination of the sample material, a clear sample preparation and the use of an experimental atmosphere with low oxygen partial pressure that contains reducing gases. If the temperature during the measurement is not sufficiently stable, peak broadening/shifting will extend the uncertainty of the peak identification, which is not considered in uncertainty analysis. If the translational frequency in z-direction is not directly determined, the peak identification has to be performed very carefully, as can be seen in Section 3.3. An overestimated density will lower the surface tension result. Using the unassigned OD evaluation method will give an upper limit for the surface tension, which is sometimes nearly identical to the results obtained by the assigned method, but sometimes significant differences can arise. Finally, the objectivity of the experimenter might have a crucial influence on the evaluation results and therefore the results should be double-checked by a colleague.

3 RESULTS AND DISCUSSION

3.1 Literature Study

The 17 investigated studies, summarized/referenced in Table 3 and plotted in Figure 6, exhibit a mean surface tension at the melting temperature of $\overline{\gamma}(T_{\text{M}}) = (1800 \pm 100)$ mN·m^{-1}.

To distinguish between the two main approaches, performing non-containerless and containerless measurements, it is evident that non-containerless methods obtain a 2% lower $\overline{\gamma}(T_{\text{M}})$ in a bandwith of only 3%, instead of 8% of $\overline{\gamma}(T_{\text{M}})$ for containerless methods. Typically, non-containerless methods should give lower results due to contamination of the highly reactive liquid melts with crucibles or other surfaces. The highly spreading results of the containerless methods can be traced back to the use of various

TABLE 3
Results of nickel literature including the year of publication, first author, experimental and evaluation method (for abbreviation see Table 1), surface tension at the melting point, temperature gradient of the surface tension, melting point stated in study and the literature reference

Year	Name	Method	$\gamma(T_M)$ / mN·m^{-1}	$\frac{\partial\gamma}{\partial T}$ / mN·m^{-1}·K^{-1}	T_M / K	Ref
1953	Kingery	SD	1735	–	–	[27]
1961	Fesenko	MBP	1777†	–0.38	–	[28]
1963	Allen	DDW	1780	–0.98	–	[29]
1969	Ayushina	SD	1770†	–0.22	–	[30]
1985	Keene	EML + OD: *R*	1854 ± 2%	–0.36	–	[7]
1986	Schade	EML + OD: *R*	1846	–0.25	1725	[9]
1986	Nogi	SD	1782	–0.34	–	[8]
1986	Nogi	EML+ OD: *R*	1845	–0.43	–	[8]
1991	Eckler	EML + OD: *CB(6.3)*	1924	–0.1	1728	[6]
1992	Sauerland	EML + OD: *CB(6.1)UA*	1868	–0.22	1728	[12]
1993	Brooks	EML + OD: *CB(5.20)UA*	1797	–0.15	1728	[14]
2004	Ishikawa	ESL + OD: *FB*	1739	–0.22	1728	[11]
2005	Brillo	EML + OD: *CB(5.20)UA*	1770	–0.33	1727	[13]
2008	Xiao	SD	1823	–0.46	1728	[31]
2014	Ozawa	EML + OD: *CB(5.20)UA*	1829	–0.4014	1728	[15]
2015	Aziz	EML + OD: *CB(5.20)UA*	1864 ± 3	–0.35 ± 0.02	1728	[1]
2016	SanSoucie	ESL + OD: *R*	1653†	–0.03558	1728	[10]

† calculated $\gamma(T_M)$ from $\gamma(T \neq T_M)$.

OD evaluation formulas. As described in Section 2.1, the early EML formulas do not consider terrestrial conditions as the formula of *Blackburn and Cummings* (1991) [5] does. By excluding those outdated studies of *Keene*, *Schade*, *Nogi*, *Eckler* and *Sauerland*, the $\bar{\gamma}(T_M)$ of all studies is lowered by 1.5%. The remaining EML studies have been exclusively obtained by *CB(5.20)UA*. The terrestrial ESL studies should generally be evaluated by the *Feng and Beard* [4] correction of the Rayleigh formula, where the drop charge and the terrestrial gravity is considered. An exception has been made at the study performed by *SanSoucie* [10] as the deviation from the *Rayleigh formula* has been estimated to be negligibly small at the ESL setup at *NASA Marshall Space Flight Center* in Huntsville.

3.2 Re-measurement of nickel at TU Graz

Surface tension has been obtained for the different supplier (*Alfa Aesar*, *Goodfellow*, *Sigma Aldrich*) in a temperature range from (1600–1870) K. In Figure 7, no significant difference for the single suppliers is evident. The results are summarized in Table 4.

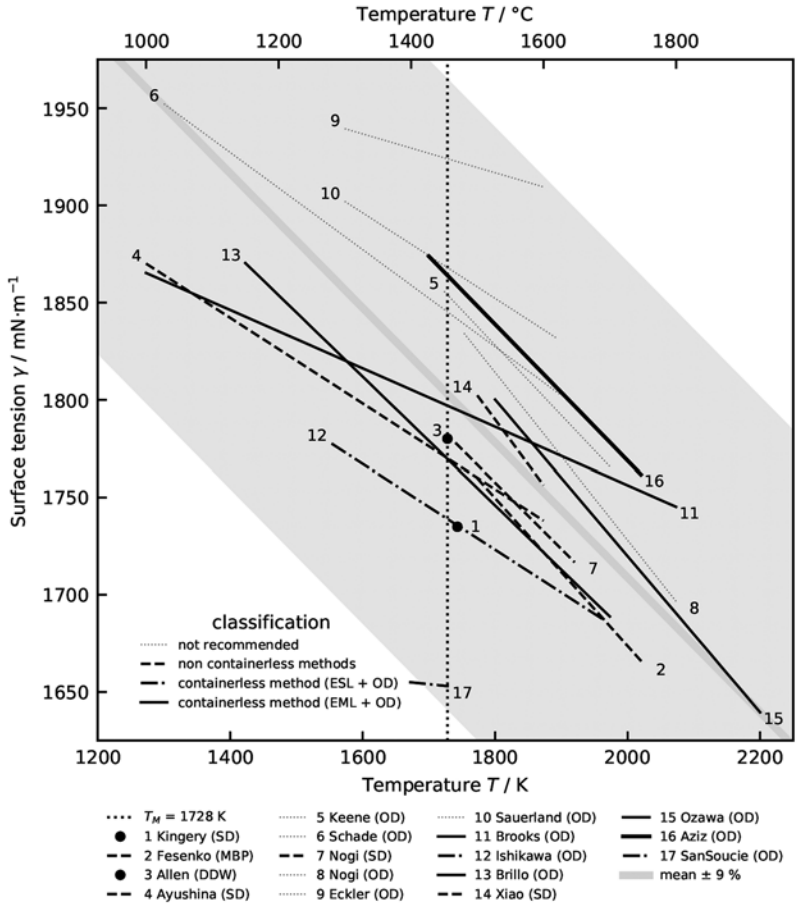

FIGURE 6
Compendium of recent studies.

The most accurate result is obtained by using the method *CB(5.20)A*, but the upper limit approximation using *CB(5.20)UA* only gives 0.2% increased results. The total uncertainty of the fit, containing fit parameter and temperature errors, calculated by GUM at the melting point is $d\gamma(T_M) = 12\ mN{\cdot}m^{-1} = 0.7\%$.

3.3 Re-evaluation of Aziz study

When comparing the measurement results of this study and the one of *Aziz* [1] performed in 2015 using nearly the same EML setup at TU Graz and partly a sample material from Alfa Aesar with the same LOT number, the results of *Aziz* are 7% higher than the one of this study. In 2016, *Aziz* claimed in his dissertation [16] that the former use of *CB(5.20)UA* significantly elevated the results in comparison to *CB(5.20)A* by 1.3%, but without stating

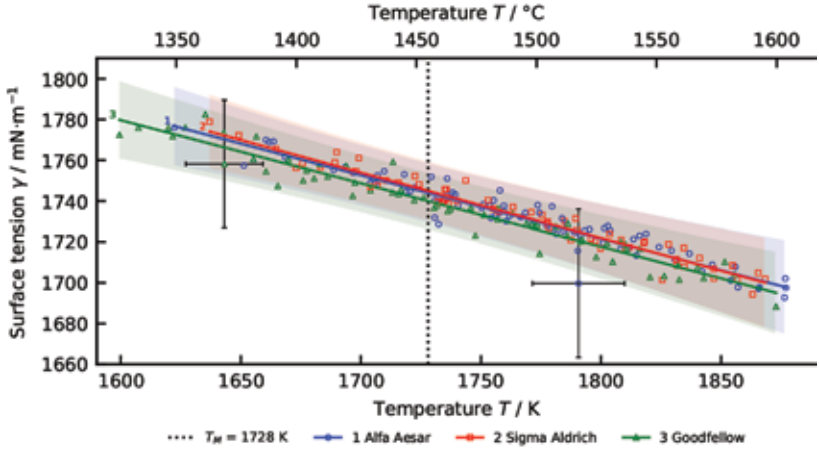

FIGURE 7
Surface tension results classified to the material supplier *Alfa Aesar*, *Sigma Aldrich* and *Goodfellow* evaluated using *CB(5.20)A*.

TABLE 4
Results of surface tension of liquid nickel provided by different suppliers with methods denoted in Table 1 according to the linear fit equation (1)

Supplier	**Method**	$\gamma(T_M)$ / mN·m^{-1}	$\frac{\partial\gamma}{\partial T}$ / mN·m^{-1}·K^{-1}
Alfa Aesar	*CB(5.20)A*	1744 ± 4	–0.31 ± 0.06
Goodfellow	*CB(5.20)A*	1740 ± 4	–0.31 ± 0.05
Sigma Aldrich	*CB(5.20)A*	1745 ± 4	–0.32 ± 0.06
all	*CB(5.20)A*	1743 ± 2	–0.31 ± 0.03
all	*CB(5.20)UA*	1746 ± 2	–0.30 ± 0.03

an exact fit equation. Fit equations based on experimental data obtained by Aziz are valid for the temperature range of (1700–2020) K.

The re-evaluation of the original data using the *CB(5.20)UA*, the same OD evaluation equation as *Aziz* used, the resulting surface tension is 5.5% lower than the original one. When using *CB(5.20)A*, the surface tension is even 8% lowered related to the original results. As depicted in Figure 8, the total difference between the re-evaluated data from *Aziz* using *CB(5.20)A* and the results of this study is with 1.3% still clearly noticeable. The results of the re-evaluation and the comparison are summarized in Table 5.

The main reason for the discrepancy between the obtained surface tension results is the differently determined translational frequency in z-direction $\nu_{\tau,z}$. *Aziz* determined it with $\overline{\nu}_{\tau,z} = (5.9 \pm 0.3)$ Hz in the same order of magnitude as $\overline{\nu}_{\tau,x} = (5.5 \pm 0.1)$ Hz and $\overline{\nu}_{\tau,y} = (5.7 \pm 0.1)$ Hz. According to *Cummings and Blackburn* [5], $\nu_{\tau,z}$ should be the double of $\nu_{\tau,x}$ and $\nu_{\tau,y}$. Through the

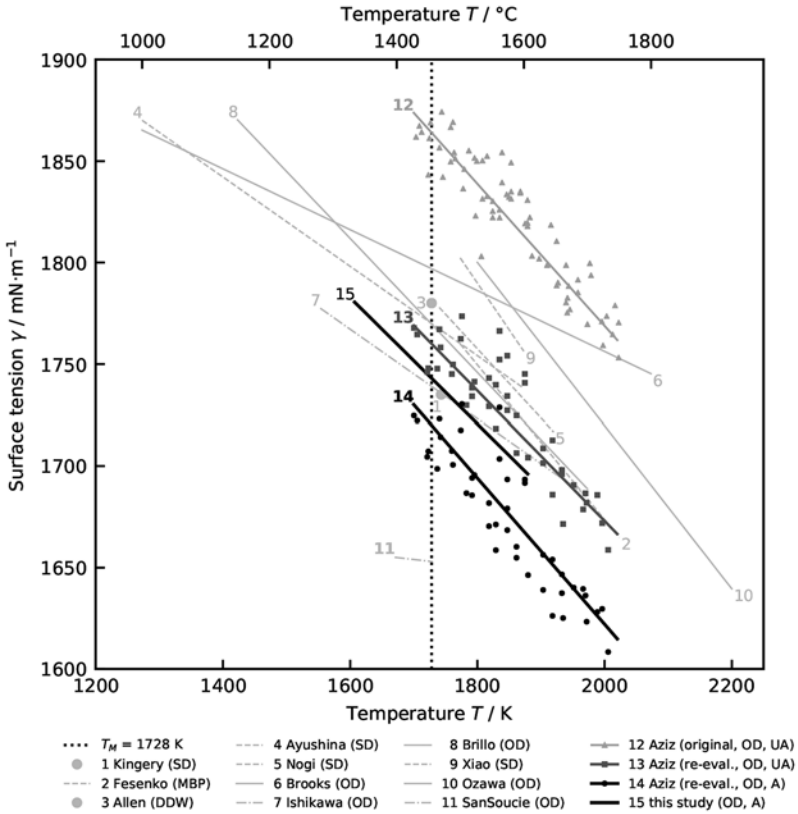

FIGURE 8
Results of the re-evaluation of the study performed by *Aziz* and comparison with this study.

TABLE 5
Summary of comparison and re-evaluation of results of *Aziz* [1]

Description	**Method**	$\gamma(T_M)$ / mN·m^{-1}	$\frac{\partial\gamma}{\partial T}$ / mN·m^{-1}·K^{-1}
Aziz (original)	*CB(5.20)UA*	1864 ± 3	–0.35 ± 0.02
Aziz (re-eval.)	*CB(5.20)UA*	1760 ± 10	–0.32 ± 0.09
Aziz (re-eval.)	*CB(5.20)A*	1720 ± 10	–0.36 ± 0.09
this study	*CB(5.20)A*	1743 ± 2	–0.31 ± 0.03

re-evaluation of the original dataset, $\nu_{\tau,z}$ has been determined as described in Section 2.3 and lies in the range of $\bar{\nu}_{\tau,z} = (14.6 \pm 0.3)$ Hz. The visualisation in Figure 9 shows the deviation of ν_R to the root mean square (rms) fundamental frequencies $\nu_{2,m}$, which is dependent on the rms translational frequency,

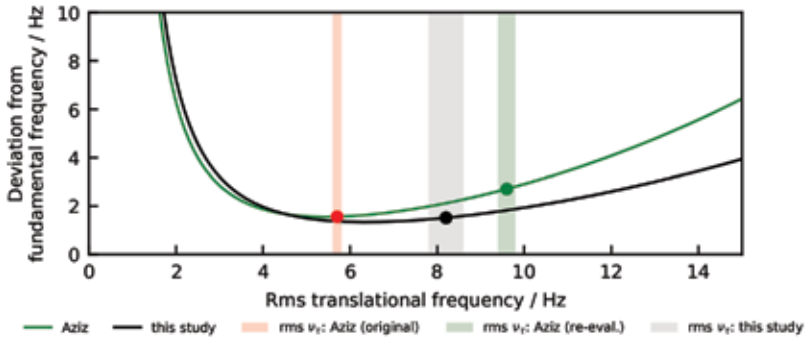

FIGURE 9
Dependency of the deviation of the Rayleigh frequeny ν_R from the fundamental frequency $\nu_{2,m} = \frac{1}{5}\left(\nu_{2,0}^2 + 2\nu_{2,|1|}^2 + 2\nu_{2,|2|}^2\right)$ from the rms translational frequency $\sqrt{\nu_\tau^2}$ according to *CB(5.20)A* for the study performed by Aziz and this work. The differently shaded areas denote the ranges of rms translational frequencies arising at evaluation.

after *CB(5.20)A* for both studies. For this purpose, the corresponding mean fundamental frequencies and radii of each studies have been used for the plot[6]. It is evident that the positive shift of the rms translational frequency through re-evaluation of $\nu_{\tau,z}$ of about 4 Hz gives an increase in deviation of roughly 1 Hz. For the case of this study, deviation values of about 1.5 Hz are emerging, which are 1.2 Hz lower than at the re-evaluated Aziz study.

Another differing parameter is the sample mass, that is with about 1200 mg twice as large as at this study. As a consequence, the oscillation frequencies occur in the low frequency range of (20 to 50) Hz. The combination of a higher mass and stronger sample rotation[7] is responsible for the immense difference of 2% of the unassigned and the assigned OD evaluation method. The residual deviation of 1.3% might be explained through the use of different sample masses in combination with different levitation coil setups. The used OD evaluation formula has been designed under assumption of a linearly changing magnetic field in z-direction. Each handmade levitation coil exhibits another deviation of this idealized assumption. Another explanation for the lower results of the re-evaluated *Aziz* study could be the occurrence of higher surface deformation amplitudes due to the double sample mass. Theoretically, samples with a larger radius r should have larger deformation amplitudes as surface effects, which grow $\propto r^2$, decrease in relation to volume effects, which increase $\propto r^3$. But this could not be verified until now, as a reliable measure for the

[6] Aziz: $\nu_{2,m} = 37$ Hz, radius $a = 3.3$ mm calculated from $\bar{m} = 475$ mg and $\bar{\rho}_{\text{lit}}(T_M) = 7800\ \text{kg·m}^{-3}$
This study: $\nu_{2,m} = 58$ Hz, radius $\alpha = 2.4$ mm calculated from $\bar{m} = 475$ mg and $\bar{\rho}_{\text{lit}}(T_M) = 7800\ \text{kg·m}^{-3}$.

[7] Aziz: $\overline{\Delta\nu}_{2,|1|} = 9$ Hz, $\overline{\Delta\nu}_{2,|2|} = 17$ Hz, $\overline{\Delta\gamma} = 52\ \text{mN·m}^{-1}$.
This study: $\overline{\Delta\nu}_{2,|1|} = 3$ Hz, $\overline{\Delta\nu}_{2,|2|} = 6$ Hz, $\overline{\Delta\gamma} = 3\ \text{mN·m}^{-1}$.

quantification of the deformation has to be found at first for terrestrial EML setups.

4 CONCLUSION

The recommended literature of the surface tension of liquid nickel can be found in Figure 10, where also the results of this study and the re-evaluated study of *Aziz* are depicted. A quantification of these results is summarized in Table 6.

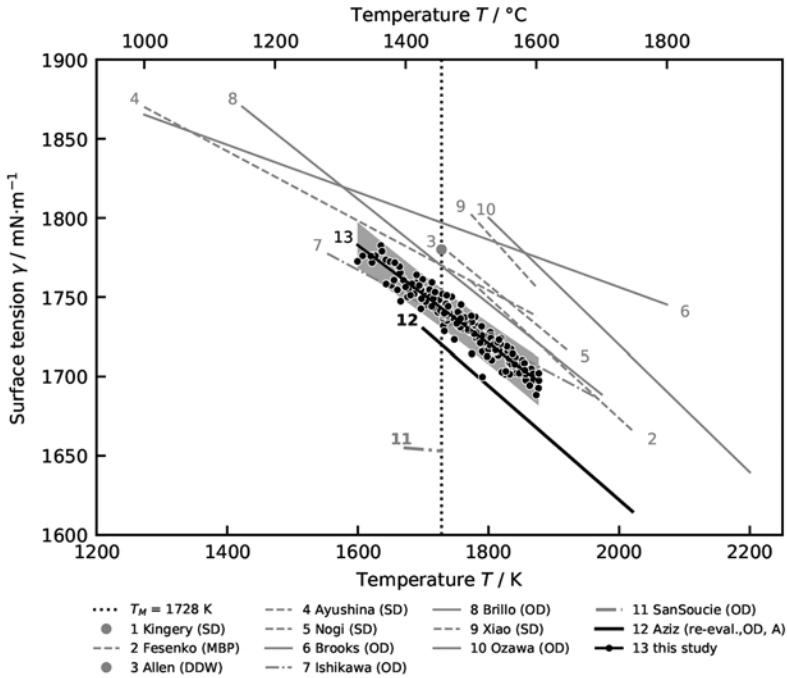

FIGURE 10
Recommended literature of the surface tension of nickel with the result of this study and the corrected results from the *Aziz* study.

TABLE 6
Summarised results of this work: Re-evaluation of Aziz results, re-measurement at TU Graz and mean of recommended literature

Description	**Method**	$\gamma(T_M)$ / mN·m^{-1}	$\frac{\partial\gamma}{\partial T}$ / mN·m^{-1}·K^{-1}	**T range**
Aziz (re-eval.)	*CB(5.20)A*	1720 ± 10	–0.36 ± 0.09	(1700–2020) K
this study	*CB(5.20)A*	1743 ± 2	–0.31 ± 0.03	(1600–1870) K
mean of recommended literature	various	1760 ± 90	–0.3 ± 0.2	(1270–2200) K

The initial guess that slight variations in the sample composition at same purity, as obtained through samples gained from different suppliers, could cause the spread in literature, could not be verified. But after the identification of literature using outdated OD evaluation formulas, the re-evaluation of the *Aziz* study and the addition of the results of this study, the spread of $\overline{\gamma}(T_{\mathrm{M}})$ has been reduced to ±5% in comparison to the initial ±7% and $\overline{\gamma}(T_{\mathrm{M}})$ has been lowered by 2%. As discussed in Section 2.3, the gained surface tension results may be increased at about 2% due to the finite deformation amplitude of oscillations. In Section 2.4 other influencing parameters with partially included uncertainty estimation are stated. Finally, to prevent misidentifications, $\nu_{\tau,z}$ should be directly obtained through an additional camera. In addition, it would be helpful to quantify the quality of a coil according to its linearity in the z-component of the magnetic field, that is presumed by the OD evaluation approach.

ACKNOWLEDGEMENTS

We are grateful to the group colleagues P. Pichler and M. Leitner for fruitful inputs and discussion. Special thanks to B. Wilthan from NIST, Boulder, for valuable impulses about obtaining high quality temperature calibration plateaus and to D. Matson from Tufts University, Medford, for drawing attention to the existence of frequency shifts for increasing surface deformation amplitudes. Work partially funded by the Austrian Research Promotion Agency (FFG), Project "Surfacetension-Steel" (Project-No. 855678). Supported by TU Graz Open Access Publishing Fund.

REFERENCES

[1] Aziz, K., Schmon, A., Pottlacher, G. *High Temp. High Press.*, **44** (2015), 475.
[2] Leitner, T., Klemmer, O., Pottlacher, G. *Tm-Tech. Mess.*, **84** (2017), 787, https://doi.org/10.1515/teme-2017-0085.
[3] Rayleigh, Lord *Proc. Royal Soc. Lond.*, **29** (1879), 71, https://doi.org/10.1098/rspl.1879.0015.
[4] Feng, J. Q., Beard, K. V. *Proc. Royal Soc. A*, **430** (1990), 133, https://doi.org/10.1098/rspa.1990.0084.
[5] Cummings, D. L., Blackburn, D. A. *J. Fluid Mech.*, **224** (1991), 395, https://doi.org/10.1017/s0022112091001817.
[6] Eckler, K., Egry, I., Herlach, D. M. *Mater. Sci. Eng. A*, **133** (1991), 718, https://doi.org/10.1016/0921-5093(91)90170-R.
[7] Keene, B. J., Mills, K. C., Brooks, R. F. *Mater. Sci. Technol.*, **1** (1985), 568, https://doi.org/10.1179/mst.1985.1.7.559.
[8] Nogi, K., Ogino, K., McLean, A., Miller, W. A. *Metall. Trans. B*, **17** (1986), 163, https://doi.org/10.1007/bf02670829.
[9] Schade, J., McLean, A., Miller, W. *Undercooled Alloy Phases*, (1986), 233.
[10] SanSoucie, M. P., Rogers, J. R., Kumar, V., Rodriguez, J., Xiao, X., Matson, D. M. *Int. J. Thermophys.*, **37** (2016), https://doi.org/10.1007/s10765-016-2085-6.

[11] Ishikawa, T., Paradis, P.-F., Saita, Y. *J. Jpn. Inst. Met.*, **68** (2004), 781, https://doi.org/10.2320/jinstmet.68.781.
[12] Sauerland, S., Eckler, K., Egry, I. *J. Mater. Sci. Lett.*, **11** (1992), 330, https://doi.org/10.1007/bf00729172.
[13] Brillo, J., Egry, I. *J. Mater. Sci.*, **40** (2005), 2213, https://doi.org/10.1007/s10853-005-1935-6.
[14] Brooks, R., Mills, K. *High Temp. High Press.*, **25** (1993), 657.
[15] Ozawa, S., Takahashi, S., Watanabe, N., Fukuyama, H. *Int. J. Thermophys.*, **35** (2014), 1705, https://doi.org/10.1007/s10765-014-1674-5.
[16] Aziz, K. *PhD thesis*. Graz University of Technology, Graz; 2016, http://diglib.tugraz.at/surface-tension-measurements-of-liquid-metals-and-alloys-by-oscillating-drop-technique-in-combination-with-an-electromagnetic-levitation-device-2016.
[17] Busse, F. H. *J. Fluid Mech.*, **142** (1984), 1, https://doi.org/10.1017/s0022112084000963.
[18] Schmon, A. Graz University of Technology, Graz; 2016, http://diglib.tugraz.at/density-determination-of-liquid-metals-by-means-of-containerless-techniques-2016.
[19] Rumble, J. *CRC Handbook Chemistry Physics, 100th Edition*. Taylor & Francis Ltd.; 2019.
[20] Henning, F. *Temperaturmessung*. Springer Science Business Media; 1977, https://doi.org/10.1007/978-3-642-81138-8.
[21] Nasch, P. M., Steinemann, S. G. *Phys. Chem. Liq.*, **29** (1995), 43, https://doi.org/10.1080/00319109508030263.
[22] Chung, S. K., Thiessen, D. B., Rhim, W.-K. *Rev. Sci. Instrum.*, **67** (1996), 3175, https://doi.org/10.1063/1.1147584.
[23] Brillo, J., Egry, I. *Int. J. Mater. Res.*, **95** (2004), 691, https://doi.org/10.3139/146.018009.
[24] Schmon, A., Aziz, K., Pottlacher, G. *Metall. Mater. Trans. A*, **46** (2015), 2674, https://doi.org/10.1007/s11661-015-2844-1.
[25] Lee, J., Matson, D. *Int. J. Thermophys.*, **35** (2014), 1697, https://doi.org/10.1007/s10765-014-1662-9.
[26] Xiao, X., Hyers, R. W., Wunderlich, R. K., Fecht, H.-J., Matson, D. M. *Appl. Phys. Lett.*, **113** (2018), 011903, https://doi.org/https://doi.org/10.1063/1.5039336.
[27] Kingery, W. D., Humenik Jr., M. *J. Phys. Chem.*, **57** (1953), 359, https://doi.org/10.1021/j150504a026.
[28] Fesenko, V. V., Vasiliu, M. I. *Poroshkovaya Metallurgiya*, (1961), 25.
[29] Allen, B. C. *T. Metall. Soc. AIME*, **227** (1963), .
[30] Ayushina, G. D., Levin, E. S., Geld, P. V. *Russ. J. Phys. Chem.*, **43** (1969), 2756.
[31] Xiao, F., Liu, L.-X., Yang, R.-H., Zhao, H.-K., Fang, L., Zhang, C. *T. Nonferr. Metal. Soc.*, **18** (2008), 1184, https://doi.org/10.1016/s1003-6326(08)60202-2.